

Dynamic correlations in symmetric electron-electron and electron-hole bilayers

R. K. Moudgil,^{1,*} L. K. Saini,² and Gaetano Senatore^{3,1,†}

¹*Dipartimento di Fisica Teorica, Università di Trieste, Strada Costiera 11, I-34014 Trieste, Italy.*

²*Department of Physics, Panjab University, Chandigarh - 160014, India.*

³*INFM - DEMOCRITOS National Simulation Center*

(Dated: October 29, 2018)

The ground-state behavior of the symmetric electron-electron and electron-hole bilayers is studied by including dynamic correlation effects within the quantum version of Singwi, Tosi, Land, and Sjölander (qSTLS) theory. The static pair-correlation functions, the local-field correction factors, and the ground-state energy are calculated over a wide range of carrier density and layer spacing. The possibility of a phase transition into a density-modulated ground state is also investigated. Results for both the electron-electron and electron-hole bilayers are compared with those of recent diffusion Monte Carlo (DMC) simulation studies. We find that the qSTLS results differ markedly from those of the conventional STLS approach and compare in the overall more favorably with the DMC predictions. An important result is that the qSTLS theory signals a phase transition from the liquid to the coupled Wigner crystal ground state, in both the electron-electron and electron-hole bilayers, below a critical density and in the close proximity of layers ($d \lesssim r_s a_0^*$), in qualitative agreement with the findings of the DMC simulations.

PACS numbers: 71.10.-w, 73.21.-b, 73.20.Qt

I. INTRODUCTION

In recent years, there has been considerable interest in the study of systems composed of two or more (equi-spaced) electron layers. The advances in the nanoscale semiconductor fabrication technology (such as the molecular beam epitaxy, the lithography techniques, etc.) have made available these electron systems in the coupled semiconductor quantum-well structures with a good control on the electron number density and the interwell spacing. A variety of new interesting phenomena have been observed, due entirely to the presence of interlayer Coulomb interactions. The stability of new fractional quantum Hall states¹ and the discovery of an insulating Wigner crystal (WC) phase², in the bilayer electron system in the presence of a perpendicular magnetic field, are some prominent examples. Theoretical^{3,4} as well as recent diffusion Monte Carlo (DMC)^{5,6} studies have predicted, even in the absence of magnetic field, the stabilization of the WC phase in the electron bilayer in the close proximity of layers $d \lesssim r_s a_0^*$ (see below for the definition of relevant parameters) at sufficiently low electron density. More precisely, the critical density for the phase transition is predicted to shift towards the higher density side as compared to the corresponding value in the case of an isolated electron layer. In the following we shall be confining our discussion to the double layer system.

Central in understanding the behavior of the layered electron systems are the intra- and interlayer many-body correlation effects. Since the early random-phase approximation (RPA) study by Das Sarma and Madhukar⁷, there have been many investigations focusing on the role of many-body correlations. The theoretical techniques used have mostly relied on the extensions to two dimensions (2D) of existing theories. Zhang and Tzoar⁸, Neilson and co-workers⁹, and Zheng and MacDonald¹⁰ have

used the mean-field approximation of Singwi, Tosi, Land, and Sjölander (STLS)¹¹ to study the effect of correlations on the various ground-state properties of an electron bilayer system. On the other hand, Kalman and co-workers¹² have incorporated correlations by satisfying the third-frequency sum rule of the density-density response function to study the collective modes. A general conclusion has emerged that the interlayer interactions add further to the importance of many-body correlations, which are already known to be very important in an isolated electron layer¹³. Both in the STLS and Kalman's group approaches, correlations enter in the theory in the form of a static local-field correction (LFC). In STLS, the LFC's are obtained numerically in a self-consistent way, while in the latter approach their calculation rely on the knowledge of accurate pair-correlation functions. The extent of validity of the STLS or other theories in the present context can be tested by making a direct comparison with the accurate DMC simulation results of Rapisarda and Senatore^{5,6}. However, no such comparison of the STLS results has been made so far. A comparative study is available only in case of an isolated electron layer¹⁴, where it has been found that the STLS theory, although providing a significant improvement over the lower order random-phase and Hubbard¹⁵ approximations, yet it fails to give an adequate description of correlations beyond $r_s > 3$. In particular, it yields negative value for the pair-correlation function (an unphysical result) at small separation for $r_s > 3$. This failure of the STLS approach also appears in the bilayer problem¹⁰. As usual, here $r_s = 1/(a_0^* \sqrt{n\pi})$ is the dimensionless density parameter, with $a_0^* = \hbar^2/(m_e^* e^2)$ the effective Bohr atomic radius and n the in-layer areal number density. m_e^* is the effective (band) mass of electron. We recall that r_s also provides a rough estimate of the in-layer coupling, as ratio of the (independent particle) potential and

kinetic energies of the system. The failure of the STLS theory at higher r_s has been traced back to its basic assumption of treating as static (i.e., time-independent) the electronic exchange-correlation hole¹⁶.

In the two-layer system, the interlayer interactions will result in an increase in Coulomb coupling as compared to that in an isolated layer at the same density. Therefore, we anticipate that the dynamics of correlations will be even more crucial in the two-layer system, with respect to an isolated layer. This forms part of our motivation for the present work. Here, we intend to examine the ground-state behavior of the symmetric electron-electron (e-e) bilayer by including dynamic electron correlation effects. To this end, we make use of the dynamic or quantum version of the STLS approach (qSTLS). The qSTLS theory embodies correlations beyond the conventional STLS approach and as an important improvement, its LFC is frequency-dependent. It should be pointed out here that the so-called qSTLS theory was originally developed by Hasegawa and Shimizu¹⁷ for the 3D electron system, and that its predictions of many-body properties, as adjudged by comparison with the MC results, are better irrespective of the dimensionality¹⁴ and the carrier statistics¹⁸. In view of the very recent DMC study of the symmetric electron-hole (e-h) bilayer by De Palo, Rapisarda, and Senatore¹⁹, we also employ the qSTLS theory to examine the ground-state properties of such system. For both the e-e and e-h bilayers we present results for the pair-correlation functions, the LFC factors, and the ground-state energy over a wide range of density and layer spacing. We also look for signs indicating an instability of the homogeneous liquid with respect to inhomogeneous phases of the charge-density-wave (CDW) and WC type. Finally, we compare our results with those of the DMC studies.

The rest of the paper is organized as follows: In Sec. II, we present in brief the qSTLS formalism for the double-layer system. Results and discussion are presented in Sec. III. In Section IV, we conclude the paper with a brief summary.

II. THEORETICAL FORMALISM

A. Model

We consider a double quantum-well structure with d as the center-to-center well separation. The carriers are electrons in one well and electrons or holes in the other, respectively for the e-e and e-h bilayer. The motion of carriers is free along the xy -plane and under the action of a double well potential profile in the z -direction. We assume that the wells are extremely narrow and the potential barriers along the z -axis are high enough so that the particles occupy only the lowest energy subband for the z motion and there is negligible overlap between the wave functions of particles in the two wells. The wells are assumed to be identical in each respect except for

the charge of carriers in the e-h bilayer. Further, the bilayer system is assumed to be embedded in a uniform charge neutralizing background. On neglecting the effect of integrating over the finite extent of the particle wave function in the z -direction, the Coulomb interaction potential among the carriers is obtained as

$$V_{ll'}(q) = \alpha_{ll'} V(q) e^{-q|l-l'|d}, \quad (1)$$

with $l = 1, 2$ the layer index and $V(q) = 2\pi e^2 / (q\epsilon_0)$ the intralayer interaction potential. Above ϵ_0 is the background dielectric constant and $\alpha_{ll'} = 1$ and $(-1)^{|l-l'|}$, respectively, for the e-e and e-h bilayers.

Apparently, the ground state of the above bilayer model will depend, apart from r_s , on the interlayer spacing d . It turns out convenient to introduce an additional coupling parameter as the ratio of the typical interlayer and in-layer Coulomb energies, namely, $\gamma = r_s a_0^* / d$. Thus, at $T = 0$, which is the case considered here, the bilayer model may be completely specified by r_s and γ (or d).

B. Density response function

In the dielectric approach, the density-density linear response function $\chi(q, \omega)$, which describes the response to an external potential $V^{ext}(q, \omega)$ that couples to the particle density, plays the role of a central quantity in determining the many-body properties of the system. For the bilayer, the linear response matrix $\chi_{ll'}(q, \omega)$ is formally defined by

$$\delta\rho_l(q, \omega) = \sum_{l'=1}^2 \chi_{ll'}(q, \omega) V_{l'}^{ext}(q, \omega), \quad (2)$$

where $\delta\rho_l(q, \omega)$ represents the induced particle density in the l th layer and $V_l^{ext}(q, \omega)$ the potential that couples to the density in the layer l . For completeness, we give in the following a very brief account of the qSTLS formulation of the density response for the two-layer system.

The equation of motion for the one-particle Wigner distribution function (WDF) $f_l^\sigma(\mathbf{r}, \mathbf{p}; t)$ (the superscript σ is the spin index) involves¹⁴, the *unknown* two-particle WDF $f_{ll'}^{\sigma\sigma'}(\mathbf{r}, \mathbf{p}; \mathbf{r}', \mathbf{p}'; t)$. Progress can however be made resorting to the STLS approximate decoupling ansatz¹¹, which in the two-layer system becomes

$$f_{ll'}^{\sigma\sigma'}(\mathbf{r}, \mathbf{p}; \mathbf{r}', \mathbf{p}'; t) = f_l^\sigma(\mathbf{r}, \mathbf{p}; t) f_{l'}^{\sigma'}(\mathbf{r}', \mathbf{p}'; t) g_{ll'}^{\sigma\sigma'}(|\mathbf{r} - \mathbf{r}'|), \quad (3)$$

with $g_{ll'}^{\sigma\sigma'}(|\mathbf{r} - \mathbf{r}'|)$ the equilibrium static pair-correlation function between carriers of spin σ and σ' in the layers l and l' . Expressing the particle density in terms of the one-particle WDF¹⁷, one readily obtains the induced density $\delta\rho_l(q, \omega)$ in the l th layer as

$$\delta\rho_l(q, \omega) = \chi_l^0(q, \omega) \left[V_l^{ext}(q, \omega) + V_l^{pol}(q, \omega) \right], \quad (4)$$

with

$$V_l^{pol}(q, \omega) = \sum_{l'=1}^2 \delta \rho_{l'}(q, \omega) V_{l' l}(q) [1 - G_{l' l}(q, \omega)] \quad (5)$$

the *dynamic* LFC factor that accounts for correlation effects among carriers in the layers l and l' . In Eq. (6), $S_{l' l}(q)$ is a static structure factor and $\chi_l^0(\mathbf{q}, \mathbf{q}'; \omega)$ the inhomogeneous Stern function given by

$$\chi_l^0(\mathbf{q}, \mathbf{q}'; \omega) = -2 \int \frac{d\mathbf{k}}{(2\pi)^2} \frac{f_l^0(\mathbf{k} + \mathbf{q}'/2) - f_l^0(\mathbf{k} - \mathbf{q}'/2)}{\omega - \hbar \mathbf{k} \cdot \mathbf{q}/m + i\eta}, \quad (7)$$

where $f_l^0(\mathbf{k})$ is the usual non-interacting Fermi-Dirac distribution function and η is a positive infinitesimal. For $\mathbf{q}' = \mathbf{q}$, $\chi_l^0(\mathbf{q}, \mathbf{q}'; \omega)$ reduces to Stern function $\chi_l^0(q, \omega)$. Using Eqs. (2), (4), and (5) the elements of the inverse of the linear response matrix are readily obtained as

$$\chi^{-1}_{l' l}(q, \omega) = \frac{\delta_{l' l}}{\chi_l^0(q, \omega)} - V_{l' l}(q) [1 - G_{l' l}(q, \omega)]. \quad (8)$$

The fluctuation-dissipation theorem, which relates the static structure factors with the imaginary part of the linear response functions as

$$S_{l' l}(q) = -\frac{\hbar}{n\pi} \int_0^\infty d\omega \text{Im} \chi_{l' l}(q, \omega), \quad (9)$$

closes the qSTLS set of equations for the density response matrix. Evidently, the response function calculation has to be carried out numerically in a self-consistent way. In view of the symmetry of the bilayer, we will have $A_{11} = A_{22}$ and $A_{12} = A_{21}$, where A refers to the general layer property.

C. Pair-correlation function and ground-state energy

The pair-correlation function $g_{l' l}(r)$ can be obtained directly from the inverse Fourier transform of the static structure factor as

$$g_{l' l}(r) = 1 + \frac{1}{n} \int \frac{d\mathbf{q}}{(2\pi)^2} e^{i\mathbf{q} \cdot \mathbf{r}} [S_{l' l}(q) - \delta_{l' l}]. \quad (10)$$

The ground-state energy E_{gs} (defined here as per particle) is determined by a straightforward extension of the

the *polarization* potential, $\chi_l^0(q, \omega)$ the density response function of non-interacting electrons in layer l (i.e., the Stern function²⁰) and

$$G_{l' l}(q, \omega) = -\frac{1}{n} \int \frac{d\mathbf{q}'}{(2\pi)^2} \frac{\chi_l^0(\mathbf{q}, \mathbf{q}'; \omega) V_{l' l}(q')}{\chi_l^0(q, \omega) V_{l' l}(q)} [S_{l' l}(|\mathbf{q} - \mathbf{q}'|) - \delta_{l' l}], \quad (6)$$

ground-state energy theorem²¹ to the two-layer system as

$$E_{gs} = E_0 + \int_0^{e^2} \frac{d\lambda}{\lambda} E^{int}(\lambda), \quad (11)$$

where $E_0 = p_F^2/(4m_e^*)$ is the kinetic energy per particle of the non-interacting system ($p_F = \hbar q_F$, is the Fermi momentum), λ is the strength of Coulomb interaction, and $E^{int}(\lambda)$ is the interaction energy per particle given by

$$E^{int}(\lambda) = \frac{1}{4} \sum_{l, l'}^2 \int \frac{d\mathbf{q}}{(2\pi)^2} \lambda V_{l' l}(q) [S_{l' l}(q; \lambda) - \delta_{l' l}]. \quad (12)$$

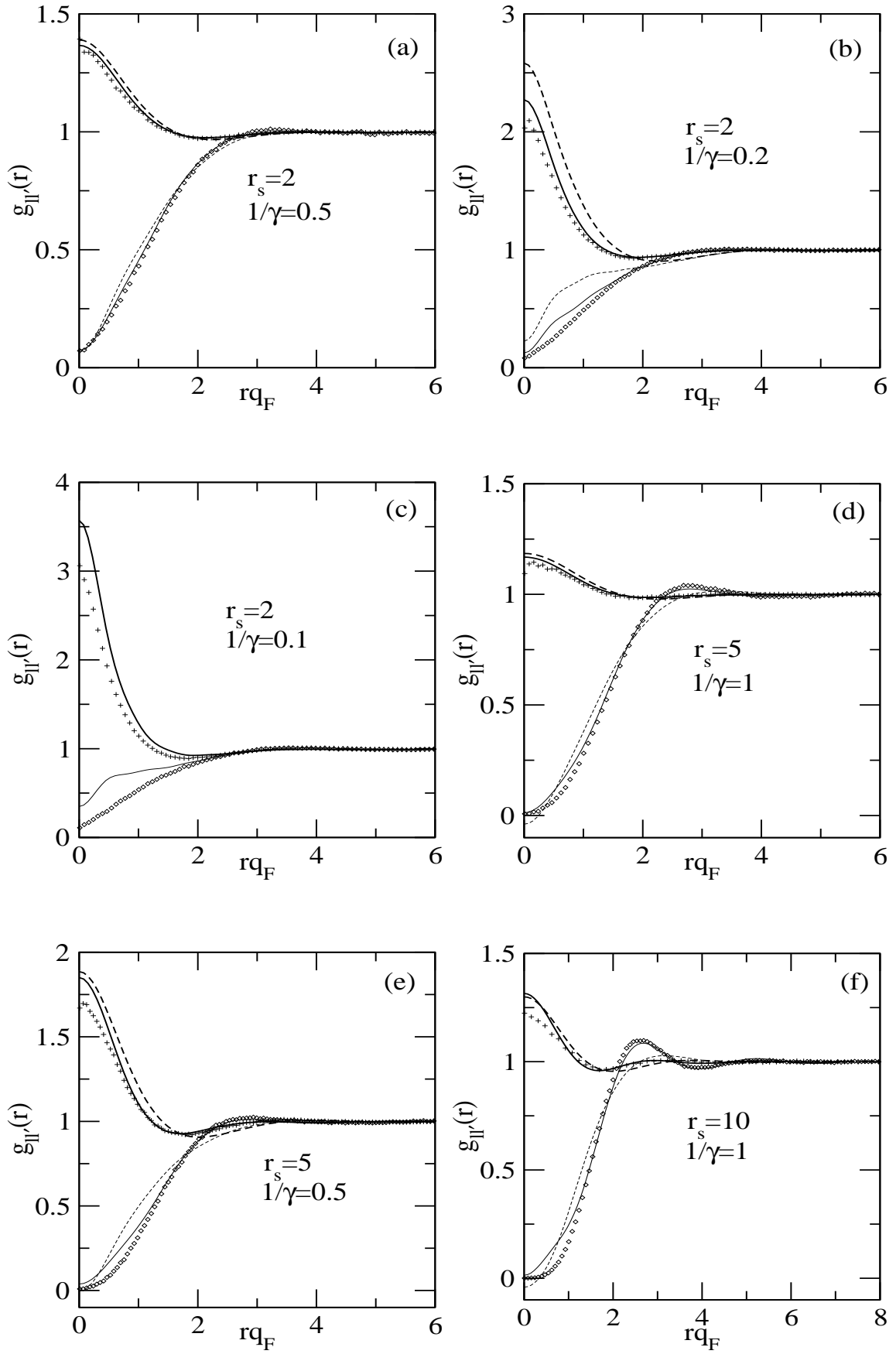
In the next section, we present results for the ground-state properties of the e-h and e-e bilayers.

III. RESULTS AND DISCUSSION

A. Pair-correlation functions

Equations (6), (8), and (9) are solved numerically in a self-consistent way for $S_{l' l}(q)$. The ω -integration in the computation of $S_{l' l}(q)$ (Eq. (9)) is performed along the imaginary ω -axis in order to avoid the problem of dealing with the plasmon poles which appear on the real ω -axis (see de Freitas et al²² and Ref.¹⁴). We accepted the solution when the convergence in $S_{l' l}(q)$ at each q in the grid of q -points was better than 0.001%. It is important to point out here that in all our calculations for the e-h bilayer we have taken $m_h^*/m_e^* = 1$ (m_h^* is the effective mass of hole).

Figures 1 ((a)-(g)) and 2 ((a)-(b)) show results for the intra- and interlayer pair-correlation functions, $g_{11}(r)$ and $g_{12}(r)$, for the e-h and e-e bilayers, respectively, at $r_s (\leq 10)$ and d values where the DMC results are available for comparison. In order to have a close comparison between the qSTLS and STLS results, the STLS curves are also depicted in the same figures. We first discuss the results for the e-h bilayer: Looking at Fig. 1 ((a)-(g)), we infer immediately that the pair-correlation functions in qSTLS are in overall better agreement with the DMC data than those in STLS. Among the notable



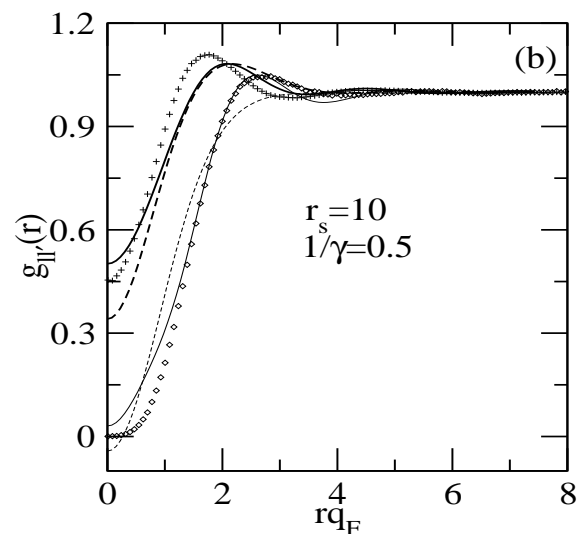
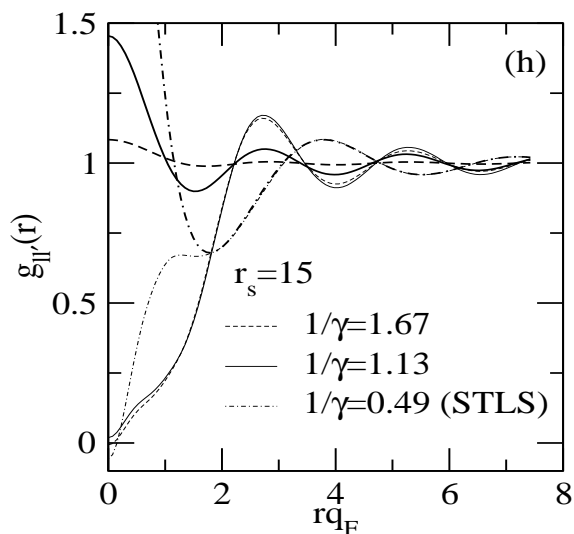
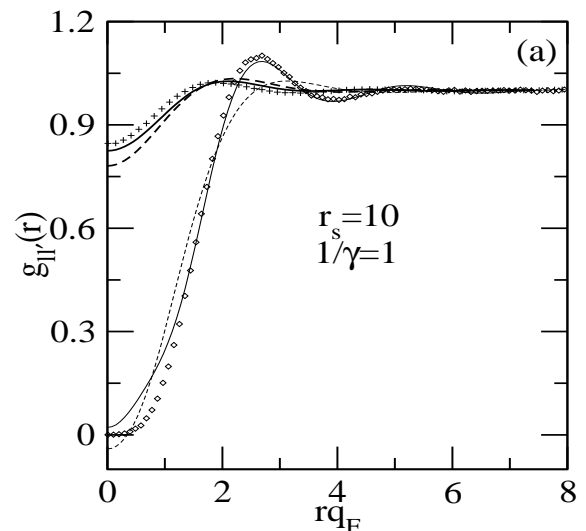
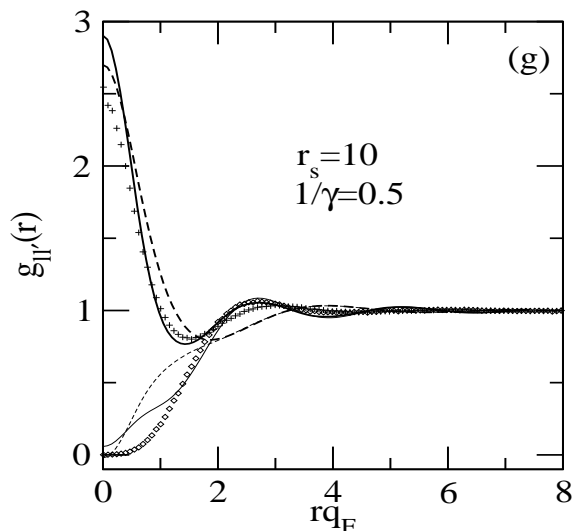


FIG. 1: (a)-(g) Pair-correlation functions $g_{11}(r)$ (thin lines) and $g_{12}(r)$ (thick lines) for the electron-hole bilayer at different values of r_s and $1/\gamma = d/r_s a_0^*$. Solid and dashed lines are, respectively, the qSTLS and STLS results; the prediction of DMC simulations^{19,23} for $g_{11}(r)$ (\diamond) and $g_{12}(r)$ ($+$) are also shown. (h) $g_{11}(r)$ (thin lines) and $g_{12}(r)$ (thick lines) at indicated r_s and $1/\gamma$ values, according to qSTLS; STLS results are shown by dash-dot lines.

features, the qSTLS theory, as a marked improvement over STLS, accounts fairly well for the oscillatory structure that develops in the DMC $g_{11}(r)$ and $g_{12}(r)$ with increasing r_s , both in terms of amplitude and period. The qSTLS $g_{11}(r)$ satisfies the positive definiteness criteria of probability for r_s up to 10, whereas the STLS $g_{11}(r)$ becomes slightly negative at small r for $r_s > 3$. We also notice that, common at each r_s , the quality of agreement between theory and DMC data somewhat diminishes for increasing values of γ . Moreover, quite similar is the trend of agreement with increasing r_s at a given value of γ ; for instance, compare $g_{11}(r)$ and $g_{12}(r)$

FIG. 2: (a)-(b) Pair-correlation functions $g_{11}(r)$ and $g_{12}(r)$ for the electron-electron bilayer; Curves are labeled as in Fig. 1. The results of DMC simulations are from Refs. 5,24.

at $1/\gamma = 0.5$ and $r_s = 2, 5, 10$. This shortcoming of the qSTLS theory seems to stem from the fact that the frequency-dependence in its LFC's represents a quantum-mechanical correction to the conventional STLS theory, while the dynamics of spatial correlations among carriers, which is expected to become vital at higher values of Coulomb coupling, is still missing. It can in fact be shown¹⁴ that the qSTLS LFC's reduce formally to the frequency-independent STLS LFC's in the limit $\hbar \rightarrow 0$.

Since decreasing d at a given r_s or increasing r_s at a given d result in an increase in the Coulomb coupling among carriers in the bilayer, the qSTLS assumption of static spatial correlations (i.e., the assumption of using static pair-correlation function in Eq. (3)) is expected to become relatively less reliable at larger values of γ or r_s . Further, we find that it becomes almost impossible

TABLE I: The ground-state energy E_{gs} per particle (in units of effective Rydberg) at different r_s and $1/\gamma$ values ($\gamma = r_s a_0^*/d$) for the e-h bilayer, according to qSTLS and STLS. DMC results are from Ref. 19.

r_s	$1/\gamma$	qSTLS	DMC	STLS
2	0.1	-0.6519	-0.6947	-
2	0.2	-0.5831	-0.6116	-0.5757
2	0.5	-0.5412	-0.5405	-0.5307
5	0.5	-0.3057	-0.3125	-0.3010
5	1.0	-0.3015	-0.3009	-0.2970
10	0.5	-0.1724	-0.1801	-0.1706
10	1.0	-0.1697	-0.1715	-0.1682
10	1.5	-0.1695	-0.1703	-0.1680

TABLE II: The ground-state energy E_{gs} per particle (in units of effective Rydberg) at $r_s = 10$ for different $1/\gamma$ values ($\gamma = r_s a_0^*/d$) for the e-e bilayer, according to qSTLS and STLS. DMC results are from Ref. 5.

r_s	$1/\gamma$	qSTLS	DMC	STLS
10	0.5	-0.1707	-0.1781	-0.1699
10	1.0	-0.1685	-0.1713	-0.1677
10	1.5	-0.1683	-0.1705	-0.1675

to obtain the self-consistent solution in both the qSTLS and STLS above a critical value of γ (r_s) at a given r_s (γ). The critical parameters are of course different in the two approaches. This is the reason that the STLS curves are absent at $r_s = 2$ for $1/\gamma = 0.1$ in Fig. 1 (c). The difficulty in obtaining the self-consistent solution, as we will see in detail in a subsequent section, is related to the instability of the system against transition to a density-modulated ground state.

For the e-e bilayer, the DMC pair-correlation functions are at present available only in the strong coupling region $r_s \geq 10$. Figure 2 ((a)-(b)) present a comparison of our results at $r_s = 10$ for $1/\gamma = 1$ and 0.5. We notice that

the qSTLS provides a reasonable estimate for $g_{11}(r)$, but it fails (together with STLS) to give a satisfactory description of $g_{12}(r)$ at $1/\gamma = 0.5$. This points once again to the importance of dynamics of spatial correlations among electrons in the e-e bilayer. The improvement over the STLS predictions is again quite noticeable.

B. Ground-state energy

The self-consistently obtained static structure factors $S_{11}(q; \lambda)$ and $S_{12}(q; \lambda)$ are used in Eq. (12) to calculate $E^{int}(\lambda)$ as a function of λ . The ground-state energy is then determined by performing the coupling-constant (λ) integration in Eq. (11). Results for the ground-state energy per particle for the e-h and e-e bilayers are given, respectively, in Tables I and II at r_s (≤ 10) and γ values where DMC data are available for comparison. The STLS results are also reported. Apparently, the qSTLS results compare more favorably with the DMC data. There is an increase in error with respect to the DMC data with increasing r_s at a given γ and with increasing γ at a given r_s , which obviously is the reflection of the behavior of the pair-correlation functions under these conditions.

C. Density-modulated ground states

The DMC studies have predicted that both the e-e and e-h bilayers will favor energetically the WC ground state above a critical value r_s^c of the in-layer coupling, at given d . We calculate here the static ($\omega = 0$) generalized susceptibility (i.e., density-density response) in the liquid phase to find out any evidence that the qSTLS theory might provide for the transition to a WC ground state. If such a transition does occur, it may appear in the static susceptibility as a divergence at the reciprocal lattice vector (RLV) of the WC lattice. Diagonalizing the density response matrix (8), the static susceptibility is obtained as

$$\chi_{\pm}(q, 0) = \frac{\chi_1^0(q, 0)}{1 - \chi_1^0(q, 0) [V_{11}(q)(1 - G_{11}(q, 0)) \pm V_{12}(q)(1 - G_{12}(q, 0))]} \quad (13)$$

The + and - signs correspond, respectively, to the in-phase and out-of-phase (π) modes of density modulations $\delta\rho(q, 0)$ in the two layers. An inspection of Eq. (13) makes it clear that $\chi_{\pm}(q, 0)$ can exhibit divergence at some q value only if the quantity within the square brackets in its denominator becomes sufficiently negative (on account of the negative sign of $\chi_1^0(q, 0)$). In an isolated layer (i.e., when $V_{12}(q) = 0$) this can happen

only if $G_{11}(q, 0)$ has values exceeding unity. However, in a bilayer^{3,9}, the interlayer interaction term can cause a divergence even if $G_{11}(q, 0)$ has values below unity. Apparently, it is the in-phase component of susceptibility that can have divergence in the e-h bilayer, while it is the out-of-phase component in the e-e bilayer. Further, as the e-h and e-e correlations are of opposite nature (i.e., $G_{12}(q, 0)$ is negative in the e-h bilayer, while it is positive

in the e-e bilayer), they will act, respectively, to support and oppose the formation of density-modulated phase (if any) in the e-h and e-e bilayers.

The static LFC factors, $G_{11}(q,0)$ and $G_{12}(q,0)$, required in the calculation of the susceptibility are determined by using the self-consistently obtained static structure factors in Eq. (6). We find quite generally that $\chi_+(q,0)$ ($\chi_-(q,0)$) exhibits for the e-h bilayer (e-e bilayer) a strong peak-structure at a finite wavevector value in the close proximity of two layers ($d \lesssim r_s a_0^*$). A critical layer separation d_c (critical r_s^c) at a given r_s (d) is encountered below (above) which it becomes almost impossible to obtain the self-consistent solution. Tracing carefully the different steps involved in the solution of the qSTLS equations, the difficulty in obtaining the convergent solution is found to be related directly to the emergence of the strong peak structure in $\chi_{\pm}(q,0)$. For $d < d_c$ at a given r_s or for $r_s > r_s^c$ at given d , a numerical instability (singularity) appears in $S_{ll}(q)$ during the iterative calculation, at a q coinciding exactly with the peak position in $\chi_{\pm}(q,0)$, while calculating $S_{ll}(q)$ from $\chi_{ll}(q,\omega)$ in Eq. (9). We find it extremely difficult to handle the instability in the self-consistent calculation and therefore, are unable²⁵ to find the convergent $S_{ll}(q)$ below (above) a critical value of d (r_s). This forbids us, in turn, to calculate $\chi_{\pm}(q,0)$ below (above) a critical value of d (r_s) at a given r_s (d). On the other hand, the emergence of a strong peak in $\chi_{\pm}(q,0)$ at a finite wavevector value followed by the numerical instability at the same wavevector during the self-consistent calculation of the density response functions could be interpreted in our theory as an indication for the onset of a phase transition from the liquid to the density-modulated ground state.

1. Electron-hole bilayer

Results for $\chi_+(q,0)$ at some selected values of r_s and d are shown in Fig. 3 ((a)-(c)). For $r_s < 5$, $\chi_+(q,0)$ has a single strong peak at small q ; for instance, at $r_s = 2$ (Fig. 3(a)) the peak is positioned at $q/q_F \approx 0.2$ and $d_c/(r_s a_0^*) \approx 0.095$. For $r_s \geq 5$, however, a second peak starts developing in $\chi_+(q,0)$ at $q/q_F \approx 2.5$, with its strength relative to that of the peak at small q/q_F growing continuously as a function of increasing r_s . At $r_s = 10$ (Fig. 3(b)), the peak at $q/q_F \approx 2.5$ eventually dominates the small- q peak and $d_c/(r_s a_0^*) \approx 0.36$. With further increase of r_s , the small- q peak disappears completely as shown in Fig. 3(c) at $r_s = 15$; $d_c/(r_s a_0^*) \approx 1.10$. The position of the peak located at $q/q_F \approx 2.5$ matches quite closely with the RLV for a triangular Wigner lattice (≈ 2.7) and therefore, we speculate that this peak signals a transition to the coupled in-phase WC ground state in the e-h bilayer. Our speculation draws further support from the fact that near the transition point $g_{11}(r)$ and $g_{12}(r)$ exhibit strong in-phase oscillations typical of an ordered phase, and this

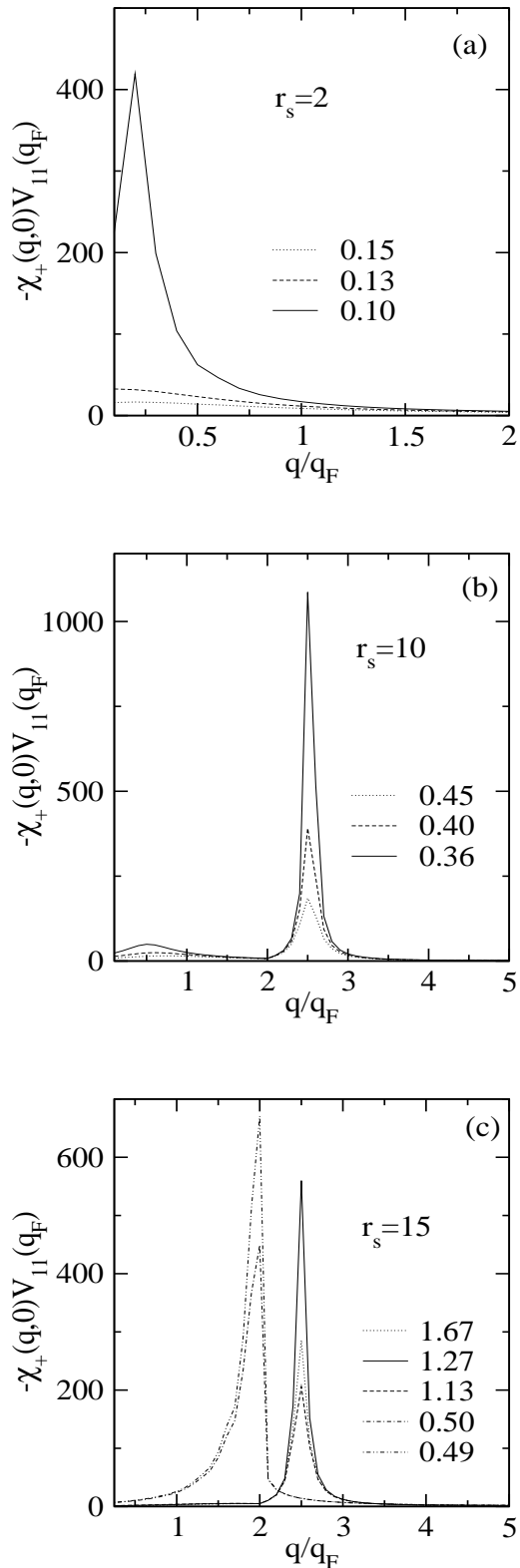


FIG. 3: (a)-(c) In-phase component of the static density susceptibility $\chi_+(q,0)$ for the electron-hole bilayer at different values of r_s and $1/\gamma = d/r_s a_0^*$, according to qSTLS. Legends indicate the values of $1/\gamma$; STLS results are shown for comparison by dash-dot lines in (c) at $r_s = 15$ and indicated $1/\gamma$ values.

feature of $g(r)$ is illustrated in Fig. 1(h) at $r_s = 15$. On the other hand, the small- q peak, whose position varies with r_s , indicates the instability of the e-h liquid against a CDW ground state. Thus, there seems to occur a crossover from a CDW to a WC ground state at a critical density $r_s^c \approx 10$. The qSTLS indication of a transition to a WC state is in agreement with the findings of the DMC study¹⁹. However, the critical r_s for the onset of the phase transition is underestimated by a factor of about 2. The qSTLS theory signals a Wigner crystallization also for an isolated electron layer, at $r_s^c \approx 17$, again with an overestimate of the critical coupling by a factor of about 2, as compared with the available DMC predictions^{5,6,26,27}. Nevertheless, an important result to note is that the electron-hole correlations in the e-h bilayer act to lower the critical r_s value, as compared to that in an isolated layer, by a factor of about 1.7, which matches closely with the DMC prediction.

Furthermore, the DMC study¹⁹ has found that the WC ground state (also, the liquid state when $r_s < r_s^c$) becomes energetically unstable against transition to an excitonic ground state as the layers of electrons and holes are brought close to each other ($d \lesssim r_s a_0^*$). There is some indication in our results, in terms of the steady buildup of $g_{12}(r = 0)$ in the close vicinity of layers, for the formation of excitons²⁸, but there is no apparent way in our theory to directly detect the transition to the excitonic ground state.

It is appropriate at this point to draw a comparison of our results with the previous work on the e-h bilayer by Liu et al⁹ and Szymanski et al⁹. Liu et al treated the correlations within the STLS approach and found at all r_s , in the close vicinity of layers, always an instability towards the CDW ground state. The STLS $\chi_+(q, 0)$ is plotted for comparison at $r_s = 15$ in Fig. 3(c); the CDW wavevector q/q_F is ≈ 2 and $d_c/(r_s a_0^*) \approx 0.48$. Also shown for comparison in Fig. 1(h) are the STLS $g_{11}(r)$ and $g_{12}(r)$ near the CDW instability (at $d/(r_s a_0^*) = 0.49$) at $r_s = 15$. On the other hand, Szymanski et al employed the STLS local-fields to include the correlation effects, but instead of carrying out the fully self-consistent STLS calculation, they fixed the intralayer LFC $G_{11}(q)$ through the MC structure factor for an isolated layer²⁶, while the interlayer LFC $G_{12}(q)$ was determined self-consistently by keeping $G_{11}(q)$ as a fixed input. Following this mixed STLS procedure, they predicted the presence of both the CDW and WC instabilities, and also a crossover from the CDW state to the WC state at $r_s \approx 15$. Thus, there is a qualitative similarity between the qSTLS results and the findings of Szymanski et al.

It is gratifying to note that the qSTLS theory seems to capture at least qualitatively the WC transition in the e-h bilayer. The breakdown of the STLS approach even at the qualitative level seems to have roots in its assumption of treating correlations through the frequency-independent (i.e., static) LFC's. To elucidate this viewpoint, the static ($\omega = 0$) qSTLS LFC's and the STLS LFC's, which in fact determine completely the behav-

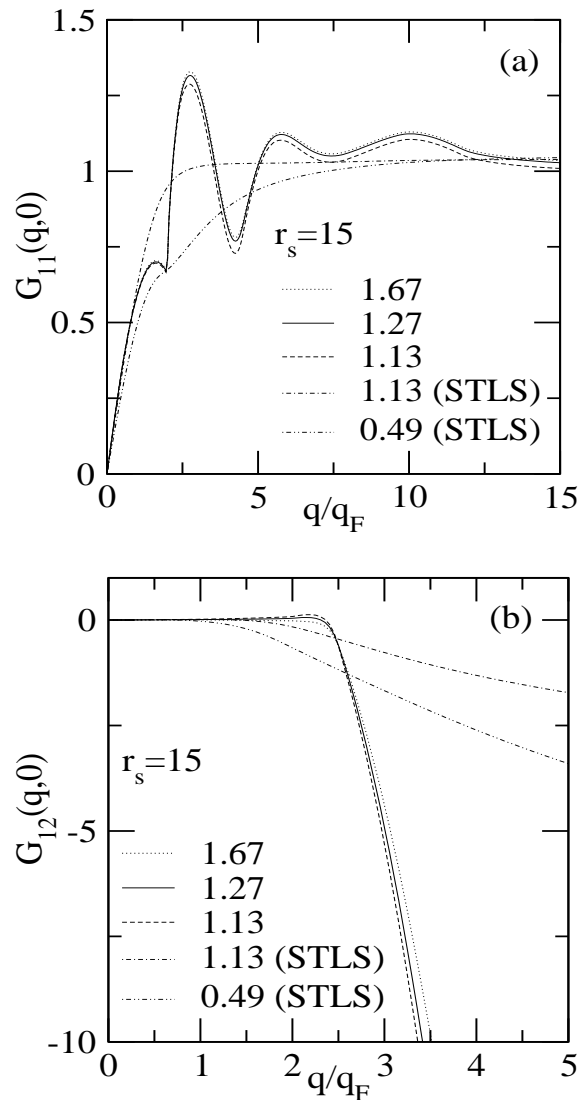


FIG. 4: Intralayer (in panel (a)) and interlayer (in panel (b)) static local-field corrections $G_{11}(q, 0)$ and $G_{12}(q, 0)$ for the electron-hole bilayer at $r_s = 15$ and different layer spacings, according to qSTLS. Legends indicate the values of $1/\gamma = d/r_s a_0^*$; STLS local-fields are also shown.

ior of $\chi_+(q, 0)$, are compared in Fig. 4 at $r_s = 15$ for different d 's. The LFC's differ markedly in the two approaches. In particular, we note that $G_{11}(q, 0)$, in contrast with the STLS $G_{11}(q)$, exhibits an oscillatory behavior, with pronounced maximum at $q/q_F \approx 3$ and with its values lying well above unity in the relevant wavevector region of $2 < q/q_F < 3$, before saturating to its limiting value of $(1 - g_{11}(0))$. Also, $G_{12}(q, 0)$ is rapidly varying in the same q -region. Consequently, the qSTLS effective static intralayer interaction, namely $[V_{11}(q)(1 - G_{11}(q, 0))]$, becomes attractive in this q -region, and this effect of $G_{11}(q, 0)$ in combination with the attractive interlayer e-h correlations gives rise to a strong peak in $\chi_+(q, 0)$ at $q/q_F \approx 2.5$. The static LFC factor exhibits a similar oscillatory behavior in an iso-

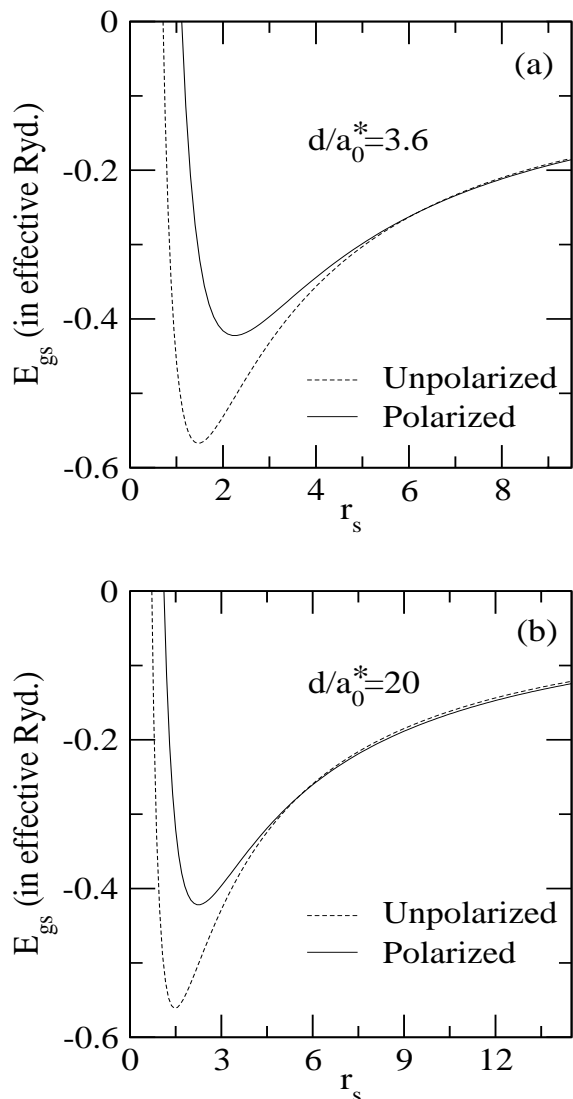


FIG. 5: (a)-(b) Comparison of the ground-state energy per particle E_{gs} between the unpolarized and polarized phases of the electron-hole bilayer at $d/a_0^* = 3.6$ (in panel (a)) and 20 (in panel (b)), according to qSTLS.

lated electron layer. Though the peaked-structure in the qSTLS static LFC factor seems to enable the qSTLS theory to capture qualitatively the WC instability, we have to mention that at least for an isolated layer such an oscillatory structure is exaggerated as compared to that found in QMC simulations²⁹.

We also examine the stability of the ground state of the e-h bilayer as a function of spin-polarization. For simplicity reasons, only two states of spin-polarization, namely the fully polarized and unpolarized (which otherwise is the case throughout the paper), are considered. A comparison between the ground-state energies of the e-h bilayer in the two states of spin-polarization (Fig. 5) reveals that a polarization transition occurs at a critical density in the liquid phase from the unpolarized to the

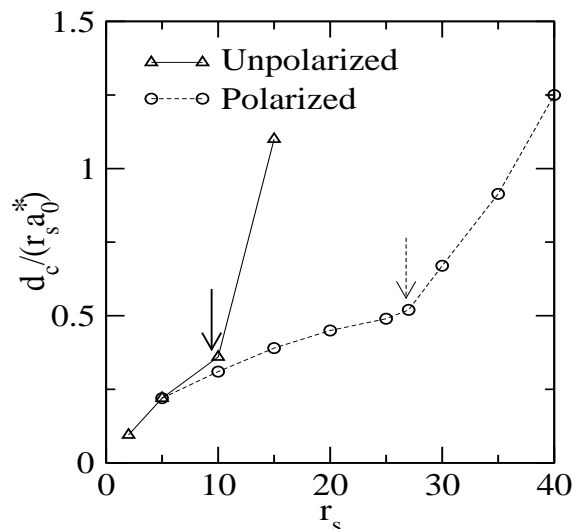


FIG. 6: Critical layer spacing $d_c/(r_s a_0^*)$ (at a given r_s) for the transition from the liquid to a density-modulated phase as a function of r_s in the unpolarized (triangles Δ) and polarized (circles \circ) phases of the electron-hole bilayer, according to qSTLS. For each case the arrows show the critical density where crossover from the charge-density-wave instability to the Wigner crystal instability occurs; The lines are just a guide for the eye.

polarized state before the unpolarized liquid could actually make transition to the seemingly WC phase. The critical density for polarization transition depends only weakly on d ; for instance the critical r_s decreases from 6 to 5.5 as d/a_0^* increases from 3.6 to 20. We emphasize here that $d/a_0^* = 3.6$ is the critical value of layer spacing at $r_s = 10$ for the WC instability. In this perspective, it becomes interesting to investigate the ground state of the polarized e-h bilayer. We find after analyzing the static susceptibility results that the qualitative behavior of the e-h ground state does not depend upon the spin-polarization. However, the crossover from the CDW phase to the WC phase now occurs at $r_s \approx 27$. The dependence of the point of instability on the spin-polarization is depicted in Fig. 6. Evidently, the critical spacing d_c in the polarized phase lies always below to that in the unpolarized phase.

2. Electron-electron bilayer

In contrast with the e-h bilayer, the interlayer correlations in the e-e bilayer tend to oppose the transition to the density-modulated phase. But, we find that this tendency of the interlayer correlations depends crucially on the rate of their growth with decreasing d , and that this rate is not strong enough to preclude transition to the density-modulated phase. We find indication for both the CDW and WC instabilities.

The $\chi_-(q, 0)$ results are shown in Fig. 7 at $r_s = 10$

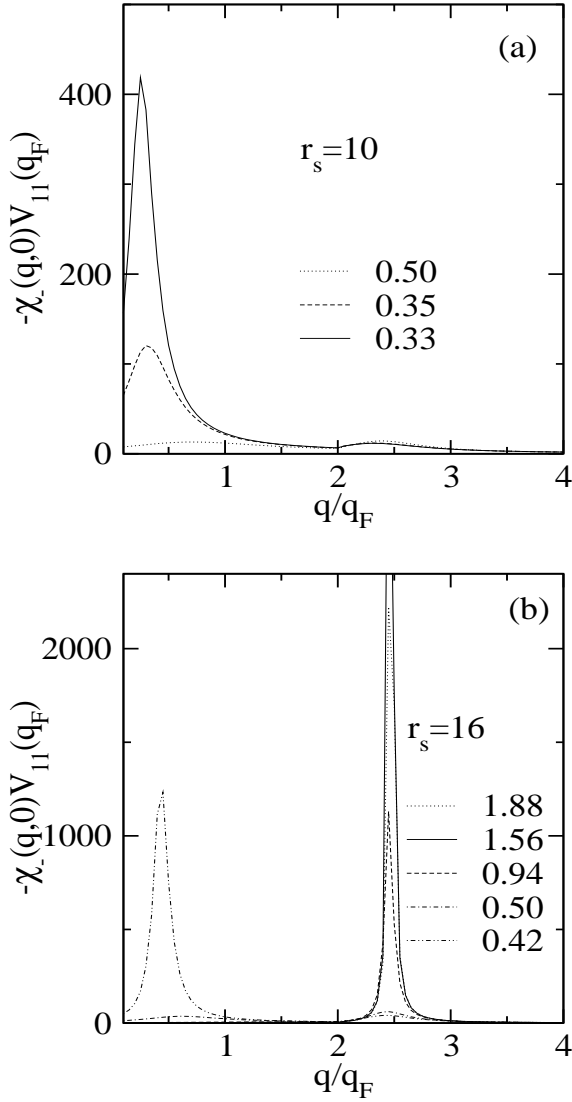


FIG. 7: (a)-(b) Out-of-phase component of the static density susceptibility $\chi_-(q, 0)$ for the electron-electron bilayer at $r_s = 10$ and 16 and different values of $1/\gamma = d/r_s a_0^*$, according to qSTLS; legends give the $1/\gamma$ values.

and 16 for some selected d 's. The CDW instability now completely dominates for r_s up to 15 . But, we notice an interesting behavior of $\chi_-(q, 0)$ at $r_s = 16$. $\chi_-(q, 0)$ exhibits a single strong peak at $q/q_F \approx 2.5$ when the layers are widely separated. The peak-height initially increases with decrease in d , nearly diverges at $d/(r_s a_0^*) \approx 1.56$, and then decreases monotonically with further decrease in d . There starts developing, however, a second peak in $\chi_-(q, 0)$ at $q/q_F \approx 0.5$ for $d/(r_s a_0^*) \leq 0.5$, and this peak eventually dominates at $d/(r_s a_0^*) \approx 0.45$ and then appears to diverge for $d/(r_s a_0^*) < 0.42$. This might possibly imply that there is a crossover to the WC ground state at $r_s \approx 16$, with the WC state however remaining stable only over a certain range of layer spacings, with a transition back to the CDW-like phase when the distance

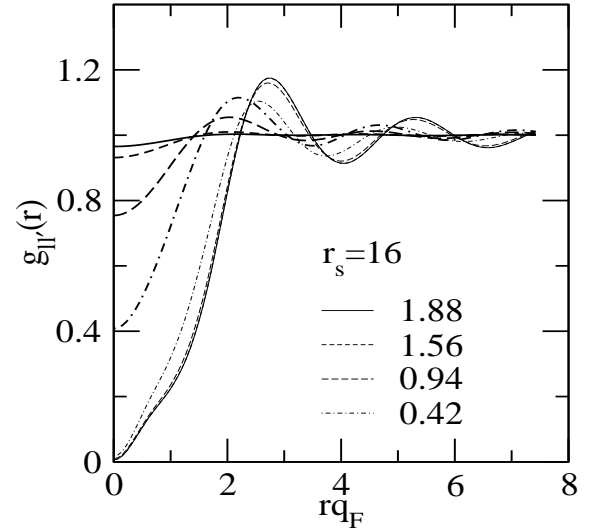


FIG. 8: Pair-correlation functions $g_{11}(r)$ (thin lines) and $g_{12}(r)$ (thick lines) in the electron-electron bilayer at $r_s = 16$ and different values of $1/\gamma = d/r_s a_0^*$, according to qSTLS. Legends give the $1/\gamma$ values. Note that the $g_{11}(r)$ at $1/\gamma = 1.88$ and at $1/\gamma = 1.56$ are practically indistinguishable.

is further diminished. The pair-correlation functions in the relevant range of d values are shown in Fig. 8. Evidently, there is a continuous decline in the amplitude of oscillation in $g_{11}(r)$ with decreasing $d/(r_s a_0^*)$ below 1.56 pointing to the obvious screening of in-layer correlations by the interlayer interactions. The present suggestion of the stability of the WC ground state in the e-e bilayer only at intermediate distances is compatible with the findings of DMC calculations^{5,6}, which for r_s not too large predict the WC phase to remain stable only at intermediate layer spacing, with the liquid phase becoming stable again at smaller spacing.

The STLS approach again does not give any indication of the WC phase transition. As in the case of e-h bilayer, this inability of STLS is a manifestation of its assumption of frequency-independent LFC's. This point is illustrated in Fig. 9 by drawing a comparison between the static qSTLS LFC's and the STLS LFC's. We notice that $G_{11}(q, 0)$ and $G_{12}(q, 0)$ both exhibit, in contrast with their STLS counterparts, a pronounced peaked-structure in the intermediate wavevector region before converging to their respective limiting values, which are close to the corresponding STLS limiting values.

D. Dynamic local-fields

We have seen above that it is the frequency-dependence of LFC's which brings in a marked difference in the qSTLS description of correlations as compared to the STLS one. Therefore, we examine the LFC's for their dependence on frequency. The results for the e-h and e-e bilayers are reported, respectively, in Figs. 10 and 11 at

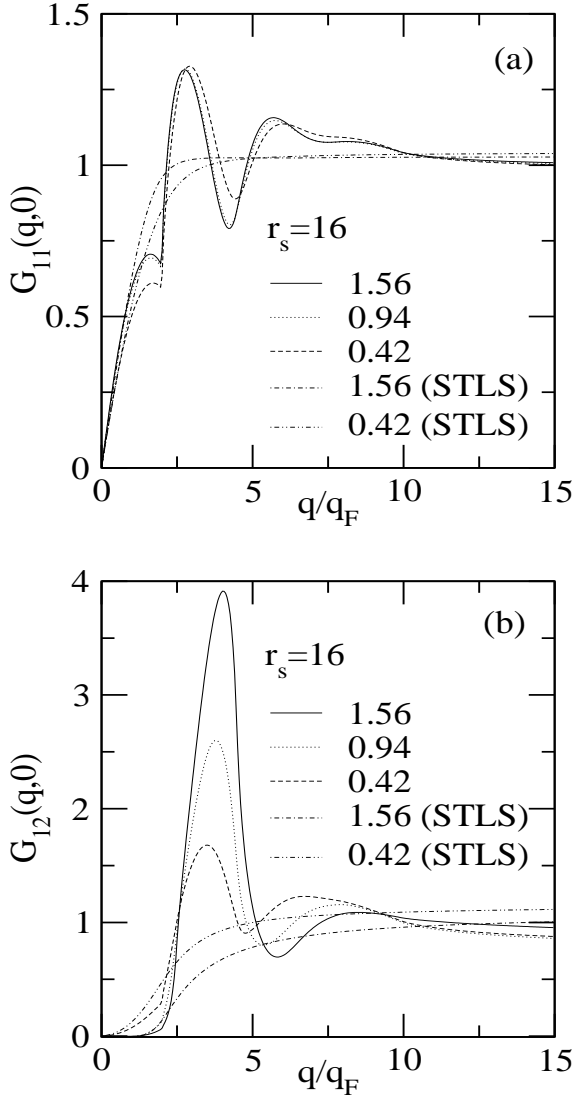


FIG. 9: Intralayer (in panel (a)) and interlayer (in panel (b)) static local-field corrections $G_{11}(q,0)$ and $G_{12}(q,0)$ for the electron-electron bilayer at $r_s = 16$ and different layer spacings, according to qSTLS. Legends indicate the values of $1/\gamma = d/r_s a_0^*$; STLS local-fields are also shown.

$q/q_F = 1.5$, $r_s = 5$, and different d' 's. The real and imaginary parts of both the intra- and interlayer LFC's are oscillatory functions of frequency - a feature which is analogous to that has been found in 3D³⁰, 2D¹⁴, and 1D³¹ electron systems. In the large frequency limit, both $G_{11}(q,\omega)$ and $G_{12}(q,\omega)$ approach formally the STLS LFC's. The LFC's in the e-h and e-e bilayers have qualitatively a similar dependence on frequency. However, we notice that, apart from the obvious difference of sign between the interlayer LFC's of the e-h and e-e layers, the attractive interlayer correlations in the former are relatively stronger in the close proximity of layers. Similar is the behavior of LFC's at other q and r_s values.

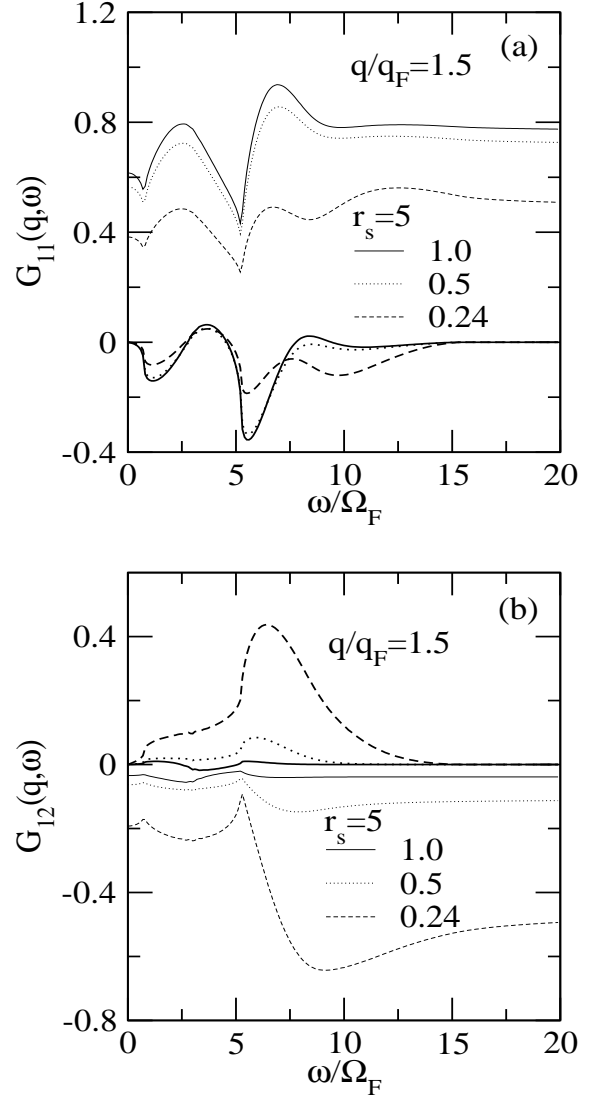


FIG. 10: Frequency-dependence of intralayer (in panel (a)) and interlayer (in panel (b)) local-fields $G_{11}(q,\omega)$ and $G_{12}(q,\omega)$ for the electron-hole bilayer at $q/q_F = 1.5$, $r_s = 5$, and different values of $1/\gamma = d/r_s a_0^*$. Thin and thick lines represent, respectively, the respective real and imaginary parts; legends indicate the $1/\gamma$ values and Ω_F is the Fermi frequency.

IV. SUMMARY AND CONCLUSIONS

In summary, we have presented a study of the ground-state behavior of the symmetric e-e and e-h bilayers by including the effect of dynamic correlations within the qSTLS theory. We have found that the inclusion of the dynamical nature of correlations introduces quantitative as well as qualitative differences in the description of many-body properties as compared to static mean-field theories of the STLS type. The qSTLS predictions for the intra- and interlayer pair-correlation functions and the ground-state energy are found to be in overall better agreement with the DMC results. The growing os-

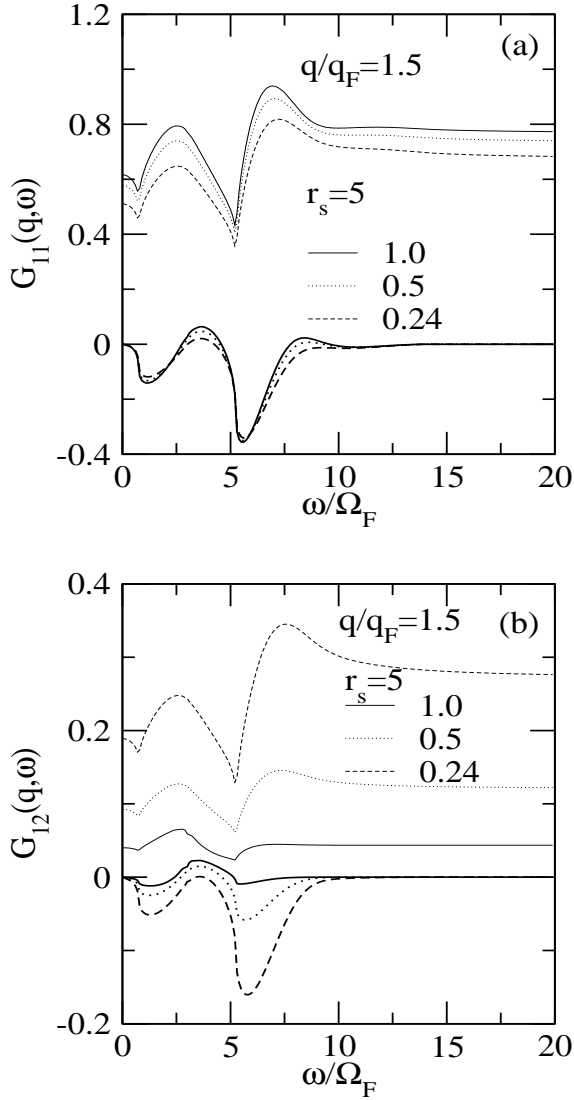


FIG. 11: (a)-(b) Dynamic local-fields for the electron-electron bilayer; Description of curves is exactly the same as in Fig. 10.

oscillatory trends in the DMC intralayer correlation function with increasing r_s are accurately reproduced both in terms of amplitude and period for $r_s \leq 10$ and $1/\gamma \geq 0.5$ - a feature that is missing in the STLS results. However, the degree of agreement with the DMC data, specifically at small interparticle separation, becomes somewhat worse with increasing $\gamma = r_s a_0^*/d$, at a given r_s or d , i.e., in the strong coupling regime. Another unique and important feature of the qSTLS theory is that, in both the e-h and e-e bilayers, it exhibits an instability towards a coupled WC ground state, below a critical density (i.e., for $r_s > r_s^c$) and in the close proximity of the layers. Moreover, at high density (for $r_s < r_s^c$) it indicates transition to a CDW ground state. Thus, a crossover from the CDW instability to the WC instability takes place at $r_s = r_s^c$. Our prediction of Wigner crystallization agrees qualitatively with the findings of the DMC calculations. However, the critical value of r_s (i.e., r_s^c) is underestimated. This discrepancy in the estimate of r_s^c seems to reflect the misrepresentation of short-range correlations at large γ or r_s in the qSTLS theory. Since the Coulomb coupling among carriers grows with increasing γ or r_s and the exchange correlations are relatively less important in the strong coupling regime, we believe that the failure of the qSTLS theory in such a regime arises from its neglect of the dynamics of the Coulomb correlations, i.e., of the Coulomb correlation hole. Another contribution to the failure is possibly due to the neglect of interaction effects on the momentum distribution function. These issues deserve further investigation.

Finally, we have also employed the qSTLS theory to examine the spin-polarization effects in the e-h bilayer. Interestingly enough, a polarization transition is found to take place from the unpolarized to the polarized liquid (at $r_s \approx 6$) well before the unpolarized liquid could actually make transition to the WC ground state. The polarized e-h bilayer too supports the CDW and WC instabilities, but the crossover density is now lowered to $r_s \approx 27$.

Acknowledgments One of us (RKM) gratefully acknowledges the financial support from the Ministero dell'Università e della Ricerca Scientifica e Tecnologica.

* On study leave from Department of Physics, Kurukshetra University, Kurukshetra- 136 119, India.

† senatore@ts.infn.it

¹ Y. W. Suen, L. W. Engel, M. B. Santos, M. Shayegan, and D. C. Tsui, Phys. Rev. Lett. **68**, 1379 (1992); J. P. Eisenstein, G. S. Boebinger, L. N. Pfeiffer, K. W. West, and Song He, *ibid* **68**, 1383 (1992).

² H. C. Manoharan, Y. W. Suen, M. B. Santos, and M. Shayegan, Phys. Rev. Lett. **77**, 1813 (1996).

³ L. Świerkowski, D. Neilson, and J. Szymański, Phys. Rev. Lett. **67**, 240 (1991); D. Neilson, L. Świerkowski, J. Szymański, and L. Liu, Phys. Rev. Lett. **71**, 4035 (1993).

⁴ G. Goldoni and F. M. Peeters, Europhys. Lett. **37**, 293 (1997); *ibid*, **38**, 319 (1997).

⁵ F. Rapisarda, *Diagramma di fase di elettroni in piani accoppiati*, PhD Thesis, University of Trieste (1996).

⁶ F. Rapisarda and G. Senatore, Aust. J. Phys. **49**, 161 (1996); *ibid*, in *Strongly Coupled Coulomb Systems*, edited by Kalman et al (Plenum Press, New York, 1998), p. 529; G. Senatore, F. Rapisarda, and S. Conti, Int. J. Mod. Phys. **B 13**, 479 (1999).

⁷ S. Das Sarma and A. Madhukar, Phys. Rev. **B 23**, 805 (1981); Also see Giuseppe E. Santoro and Gabriele F. Giuliani, Phys. Rev. **B 37**, 937 (1988); **37**, 8443 (1988).

⁸ Chao Zhang and Narkis Tzoar, Phys. Rev. **A 38**, 5786 (1988).

⁹ Lerwen Liu, L. Świerkowski, D. Neilson, and J. Szymański, Phys. Rev. **B 53**, 7923 (1996); J. Szymański, L.

- Świerkowski, and D. Neilson, Phys. Rev. **B 50**, 11 002 (1994).
- ¹⁰ Lian Zheng and A. H. MacDonald, Phys. Rev. **B 49**, 5522 (1994).
- ¹¹ K. S. Singwi, M. P. Tosi, R. H. Land, and A. Sjölander, Phys. Rev. **176**, 589 (1968); K. S. Singwi and M. P. Tosi, Solid State Phys. **36**, 177 (1981).
- ¹² Dexin Lu, K. I. Golden, G. Kalman, Ph. Wyns, L. Miao, and X. L. Shi, Phys. Rev. **B 54**, 11 457 (1996); For more recent work, see G. Kalman, V. Valtchinov, and K. I. Golden, Phys. Rev. Lett. **82**, 3124 (1999) and also see the references given therein.
- ¹³ M. Jonson, J. Phys. **C 9**, 3055 (1976).
- ¹⁴ R. K. Moudgil, P. K. Ahluwalia, and K. N. Pathak, Phys. Rev. **B 51**, 1575 (1995); **52**, 11945 (1995).
- ¹⁵ J. Hubbard, Proc. R. Soc. London Ser. A **243**, 336 (1957).
- ¹⁶ D. Neilson, L. Świerkowski, A. Sjölander, and J. Szymański, Phys. Rev. **B 44**, 6291 (1991).
- ¹⁷ T. Hasegawa and M. Shimizu, J. Phys. Soc. Jpn. **38**, 965 (1975).
- ¹⁸ K. Tankeshwar, B. Tanatar, and M. P. Tosi, Phys. Rev. **B 57**, 8854 (1998).
- ¹⁹ S. De Palo, F. Rapisarda, and G. Senatore, Phys. Rev. Lett. **88**, 206401 (2002).
- ²⁰ F. Stern, Phys. Rev. Lett. **18**, 546 (1967).
- ²¹ See, for example, G. D. Mahan, *Many-Particle Physics*, 2nd ed. (Plenum, New York, 1990).
- ²² U. de Freitas, L. C. Ioriatti, and N. Studart, J. Phys. **C 20**, 5983 (1987).
- ²³ S. De Palo and G. Senatore, private communication.
- ²⁴ G. Senatore, private communication.
- ²⁵ In fact, while we were completing the present calculations, we have been able to devise a manner to handle the resurgence of divergent peaks in the response functions, so that we are now able to perform converged calculations for values of the physical parameters r_s and d near and even inside the instability region.
- ²⁶ B. Tanatar and D. M. Ceperley, Phys. Rev. **B 39**, 5005 (1989).
- ²⁷ C. Attaccalite, S. Moroni, P. Gori-Giorgi, and G. B. Bachelet, Phys. Rev. Lett. **88**, 256601 (2002).
- ²⁸ Lerwen Liu, L. Świerkowski, and D. Neilson, Physica **B 249-251**, 594 (1998).
- ²⁹ S. Moroni, D. M. Ceperley, and G. Senatore, Phys. Rev. Lett. **69**, 1837 (1992); G. Senatore, S. Moroni, and D. M. Ceperley, in *Quantum Monte Carlo Methods in Physics and Chemistry*, edited by M. P. Nightingale and C. J. Umrigar (Kluwer Academic, Dordrecht, 1999), p. 183.
- ³⁰ A. Holas and Shafiqur Rahman, Phys. Rev. **B 35**, 2720 (1987).
- ³¹ B. Tanatar and C. Bulutay, Phys. Rev. **B 59**, 15019 (1999).